

Shear Origin of Tension in Excavation-Induced Fractures

Brian G. White

Steve Iverson

Mark Larson

Spokane Research Laboratory, National Institute for Occupational Safety and Health, Spokane, WA

ABSTRACT

The authors hypothesize that excavation-induced extension fractures are caused by elastic shearing displacement that in turn causes tension oblique to a propagating shear zone. Such extension is manifested as tension on scales larger than that of microcracks. En echelon fracture patterns are a common result. FLAC modeling confirmed that localized tension is created near the corners of mine openings. In the model, tension was concentrated at the leading edge of a simulated fracture in a pattern that could promote the formation of an en echelon fracture. Particle Flow Code models confirm progressive formation of en echelon tensile failures with distance from an opening. The elastic displacements and the resulting fractures facilitate reduction in applied load at the expense of shear deformation and lateral dilation. Understanding the mechanics of fracture and deformation is vital for designing more effective ground support practices, a major objective of ground control research being conducted at the Spokane Research Laboratory of the National Institute for Occupational Safety and Health.

1 INTRODUCTION

Excavation-induced extension fractures are common in both deep hard-rock mines and coal mines and in shallow mines in weak rock. Such fractures play a major role in roof falls, support failures, and rock bursts. However, the mechanics of their formation is not well understood despite a century of consideration.

The mechanics of extension fracture formation first received widespread attention during the 1960's. In one of a number of important papers from

that period, Fairhurst and Cook (1966) commented that these fractures form parallel to the direction of maximum compression and “represent the principal mode of macroscopic fracture in brittle rock.” They stated that “such failure may be explained on the basis of the extension of Griffith flaws . . . , [which] provides in general principle the most satisfactory explanation of brittle rock failure.” Emphasis on the formation of macroscopic excavation zone extension fractures from extending Griffith flaws has continued to the present, despite no observational evidence for such a mechanism (Lajtai et al., 1990) and the known capability of several materials, such as glass, to fail

despite a lack of development of microcracks at conditions near failure (Swanson, 1986). Several other mechanisms for the formation of microcracks have been proposed (e.g., Kemeny and Cook, 1991), but the mechanical basis for the transition from microcracks (microscopic to submicroscopic fractures) to macrofractures (typically decimeter- to meter-long fractures) has not been clearly identified.

Fairhurst and Cook (1966) also suggested that extension microfractures first form an “incipient cleavage” and that the cleavage develops into macrofractures through macroscale buckling. This idea appears to have captured little attention. Instead, the emphasis has remained on the development of macrofractures as individual entities that grow from tension generated on a microscale at fracture tips.

In contrast to these prevailing ideas, White (2002) proposed that fracture initiation and elongation are caused by elastic displacement involving combined shear and dilation. According to White, these displacements create macroscale regions of tensile stress, suggesting that Fairhurst and Cook were fundamentally correct in proposing that macrofractures are ultimately the result of macromechanics. However, in White’s proposal, the requisite macromechanics primarily involve shearing displacement rather than buckling, and excavation-induced macrofractures are both initiated by and propagate from such displacement. This paper expands upon this hypothesis to describe the formation of fractures.

Although this paper emphasizes the formation of fractures in underground hard-rock mines, the mechanism described should be active in all excavation settings that cause localized strain concentrations of sufficient magnitude to cause fracturing. Since clay has often been used in laboratory investigations of fractures (e.g., Cloos, 1955), soil exposed in trenches and soil cuts may also initially fail through fracturing. Hence, the mechanism described here is applicable to trenches, roadcuts, and pit walls, as well as excavation damage zones involving roofs, ribs, and pillars. Other rock behavior that may also be directly related to fracture zones formed through this process include strain-type rock bursts, destressing by blasting, squeeze of mine openings, coal mine gob development and subsidence, and major mine seismicity.

A well-developed understanding of the mechanics of fracturing and deformation is vital for designing more effective ground support practices and for developing and carrying out more effective research programs directed toward this end. Reduction of rock failure injuries is a major objective of ground control research currently being conducted at the Spokane Research Laboratory of the National Institute for Occupational Safety and Health (NIOSH).

2 PRIMARY AND SECONDARY FRACTURES

Carter et al. (1991) categorized extension fractures that form in the vicinity of circular openings as either primary or remote. “Primary” fractures form close to the opening and include fractures that lie parallel to the edges of the opening, which is the fracture type considered by Fairhurst and Cook (1966). “Remote” fractures form at some distance from circular openings and do not trace the shape of the opening, they apparently result from a larger-scale change in conditions caused by the presence of the opening.

A series of papers have documented the mechanics of formation of remote fractures about circular openings. Prior to the widespread use of continuum modeling, Hoek (1964) used photoelastic film to demonstrate the presence of remote areas of tension about a circular opening. Hoek and Brown (1980) found that an isolated “tension fracture” would form in each region of tension. Carter et al. (1991) successfully modeled these areas of tension using ANSYS, a finite-element program created by Swanson Analysis Systems, Inc., Canonsburg, PA.¹ However, in laboratory demonstrations of fracture development, Carter et al. noted that each initial remote fracture was succeeded by a second fracture parallel to and offset from the previous fracture in an en echelon pattern. Since en echelon fractures are typically interpreted as indicating the presence of shearing displacement, these patterns suggest that shearing displacement played a role in development of the fractures.

Fakhimi et al. (2002) repeated this exercise with circular holes using Itasca Consulting Group’s Particle Flow Code (PFC) modeling program and

¹The mention of specific products and manufacturers does not imply endorsement by the National Institute for Occupational Safety and Health

testing the equivalent laboratory specimens under confining pressure. In the test, narrow faults formed at an oblique angle to the direction of greatest stress, confirming that shear was involved in deformation at remote sites. The PFC model showed a narrow zone of abrupt change in displacement trajectories corresponding closely to the line of faulting in the sample. Fakhimi et al. noted that displacement along this zone involved shear. Hence, both continuum and PFC modeling and laboratory experience confirm the involvement of shearing displacement and macroscopic tension in the development of remote fractures about circular openings.

3 EN ECHELON EXTENSION FRACTURE ZONES

Observations in mines (White, 2002), in the laboratory (Peng and Johnson, 1972; Carter et al., 1991), and in geologic field studies (Segall and Pollard, 1983) indicate that extension fractures are commonly arranged in en echelon sets. White (2002) described the site of a face strain rock burst in a hard-rock mine and called attention to closely spaced fractures concentrated at the periphery of the burst cavity. White concluded that these fractures were arranged in an en echelon distribution, with each fracture extending only part way across the face. This pattern contrasted with that proposed by Fairhurst and Cook (1966), that fractures should extend entirely across the face. White noted the similarity of the fractures to ones seen in laboratory samples when sample ends were restrained against expansion. He also noted that the fractures resembled those involved in hourglassing of pillars (as inferred from Fairhurst and Cook, 1966) and in roof failures in a western U.S. longwall coal mine. Here, we note that en echelon fracture zones are also common geologic structures, both in the form of joints or joint zones and as the host structures for gash veins.

Field and laboratory observations emphasize that en echelon fracture zones are characterized by shearing displacement having a consistent direction with respect to the pattern of fractures. For example, rock bolts are systematically bent where they cross these fractures zones (White, 2002), geologic markers are

displaced (White and Whyatt, 1999²), and zones of en echelon fractures in laboratory samples are activated as faults that cut across individual fractures (Peng and Johnson, 1972). In an rare opportunity to examine roof fractures along the length of a crosscut, Terrill and VandelKraats (1997) and Francke et al. (1997) identified en echelon fractures that were integral to faults that extended upward toward the center of the opening from opposite edges of the roof. "Shear ruptures," which are mining-induced faults documented in South African gold mines (Gay and Ortlepp, 1979), also involve extension fractures distributed en echelon along faults that have the usual orientation with respect to the sense of displacement on the fault. We have seen numerous examples of brecciation, comminution, and faulting in both mining-induced en echelon fracture zones in the deep mines of the Coeur d'Alene Mining District and in geologic joint zones, supporting the view that shearing is fundamental to the mechanics of formation and function of these fracture zones.

Field observations suggest that the fracture zones are probably initiated near the corners of rectangular mine openings. Continuum models consistently identify regions of concentrated normal and shear stress (Hoek and Brown, 1980) and high extension strain (Stacey, 1981) at these locations. The additional fractures that define the fracture zone evidently form in succession within a propagating, oblique zone of high shear strain that extends progressively deeper and away from the opening. These observations imply that shearing is involved in the formation of primary as well as remote fractures.

The interpretation that shear is involved in the formation of en echelon fractures suggests that the fractures somehow resulted from distortion that takes place prior to fracturing. We note that simple shear causes extension between two opposite corners of deformed reference rectangles, or parallelograms. Furthermore, such extension increases continuously as shearing displacement increases. Stacey (1981) noted that high extension strain favors rock failure, although he did not provide an explanation for why

²White and Whyatt (1999) noted that zones of closely spaced mining-induced fractures often show evidence of shearing as manifested in offsets in geologic markers such as veins. These fracture zones are now interpreted as being composed of en echelon fractures.

fractures formed. For remote fractures, extension (and shear) apparently proceeds until tension is generated. Since primary fractures also form en echelon zones, it is reasonable to speculate that these also result from local tension generated by shear.

4 TENSILE ORIGIN OF PRIMARY FRACTURES

Conventional continuum models typically use fairly large modeling elements that yield consistent, reasonable results that satisfy our major interests. But, unlike models of remote fractures about circular openings, continuum models of rectangular openings generally do not identify tensile regions. On the chance that small areas of tension may be concealed by usual models having coarse element meshes, we modeled progressively narrower elements near the corner of a rectangular opening using the computer program FLAC (Fast Lagrangian Analysis of Continua) (Itasca, 1993).

We first constructed a continuum model and initialized a mesh with a 2:1 ratio of horizontal to vertical stress at the center of the grid. Gravity effects were accounted for. For convenience, the stress levels were set unrealistically high (414 MPa horizontal compressive stress and 207 MPa vertical compressive stress [60,000 and 30,000 psi, respectively]), but only linear elastic behavior was allowed. Therefore, significant ground distortion was likely, despite an absence of strain softening from the microfracturing that characterizes deformation in actual rock. We removed zones to form a rectangular opening 6.1 m wide by 4.3 m high (20 by 14 ft) at the center of the grid and monitored the effects of excavation. Boundaries were placed 18 m (60 ft) from the opening to minimize their influence near the opening. To see if we could find tension that would otherwise be hidden, the grid size was kept small; zone size was 7.6 m wide by 7.6 cm high (3 by 3 in). However, for 0.6 m (2 ft) above the opening, zone height was reduced to 1.9 cm (0.75 in).

Figure 1A shows principal stresses as hatch marks in the upper left roof of the opening. Two areas of tension are identified; these areas are shown more clearly in a contour plot of least principal stress (figure 1B). For clarity, the tensile areas are traced by lines drawn freehand. The location with

the greatest tensile stress (about 35% of the applied horizontal stress of 207 MPa (30,000 psi) is located in the roof about 13 cm (5 in) from the corner and close to the skin of the opening. If tensile stress at this location exceeds tensile strength, formation of a tension fracture is guaranteed. In our example, the calculated tension exceeds the tensile strength of all rock types. Hence, an origin of primary fractures from physical tension is a reasonable interpretation.

In another FLAC simulation, a “glued” interface (in which opposite nodes were not allowed to separate from each other) traversed the model 7.6 cm (3 in) above the opening. Thin elements were placed below the interface and above the horizon of the opening, and the same internal stresses and boundary conditions were applied as in the example above. Figure 1C shows contours of least principal stress and the location of the glued interface. This view is enlarged in comparison to figure 1B so that the rib is located 6.4 cm (2.5 in) to the left of the edge of the plot. Similar tensile zones are present to compare to the case of no interface, except that the right tensile zone is slightly higher. We suggest this occurred because we initialized the interface with no normal stress. Even so, the result is close enough to the continuum case to consider them practically equivalent.

The interface was then “unglued” from 7.6 to 23 cm (3 to 9 in) to the right of the rib line to simulate a fracture parallel to the edge of the opening. Figure 1D shows the contours of minimum principal stress along with the location of the unglued portion of the interface (shown by x’s connected by lines). Ungluing the interface caused the tensile zone to extend further above and to the right. The greatest tensile stress above the interface is 1.7% of the maximum applied stress, or 5 MPa (720 psi). Figure 1E shows results with the unglued portion extending from 7.5 to 53 cm (3 to 21 in) to the right of the rib and indicates that the area of tension expands upward and advances to the right as the simulated fracture is extended. The maximum tensile stress above and to the right of the fracture was about 8% of the maximum applied stress, or 30 MPa (5000 psi). This indicates that the likelihood of an en echelon fracture forming increases as the simulated fracture grows.

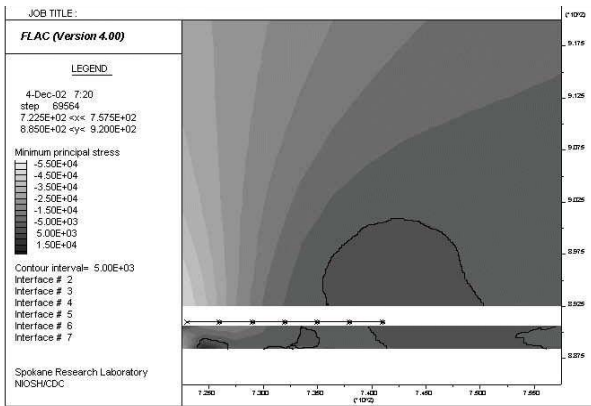
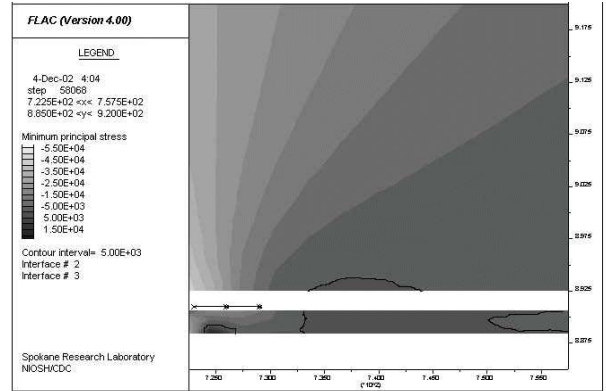
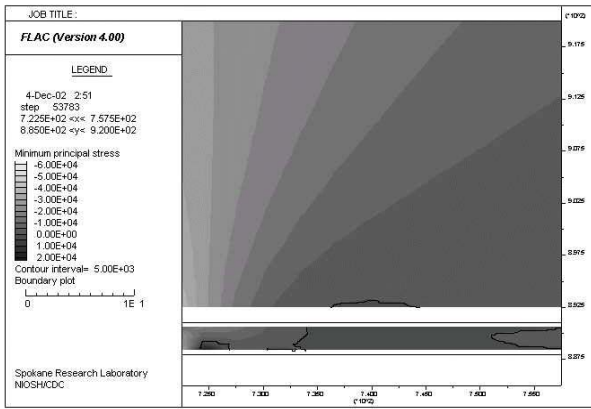
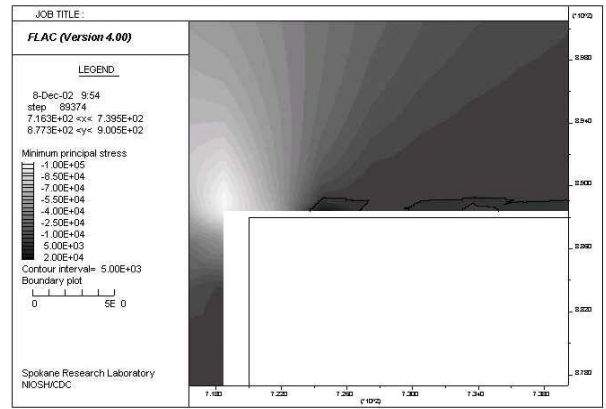
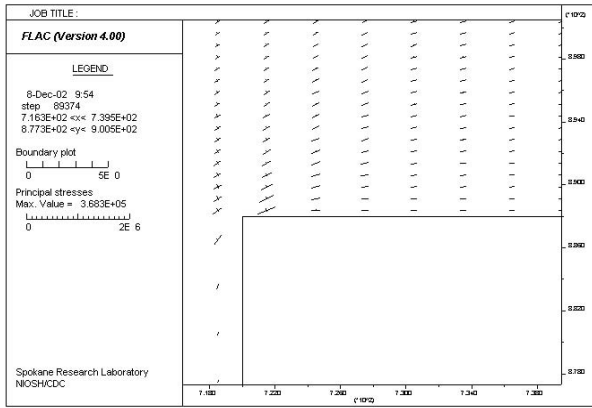


Figure 1.— Stages in crack formation. *A*, *Top left*, Principal stresses in the upper left roof of the opening shown as hatch marks; *B*, *top right*, minimum principal stress. Tensile regions are highlighted by hand. The region of greatest tension is nearest the corner; *C*, *center left*, “glued” interface (in which opposite nodes were not allowed to separate from each other) 7.6 cm (3 in) above the opening. Interface is progressively unglued in subsequent figures; *D*, *center right*, interface “unglued” from 7.6 to 23 cm (3 to 9 in) to the right of the rib line to simulate a fracture parallel to the edge of the opening; *E*, *bottom left*, Interface unglued from 7.5 to 53 cm (3 to 21 in) to the right of the rib. Note that region of tension expands upward as the simulated fracture is extended, favoring formation of an en echelon fracture.

We also duplicated this exercise with PFC2D (Itasca, 1999). A test was designed to simulate conditions along one side of a rectangular mine opening using the biaxial test simulation provided by Itasca (Itasca, 1999). To simulate a rock mass, circular particles were generated in a tightly packed assemblage and bonded together using parallel bonds. These bonds acted like glue and had stiffness and strength properties in both normal and shear. Table 1 lists the important input parameters used in the simulation.

Table 1. PFC Input parameters.

Input	Value
Particle radius (minimum, maximum)	3.00e-4, 4.98e-4 m
Mean particle density	2360 kg/m ³
Bond strength	200 MPa
Standard deviation	0.5e6 MPa
Modulus of elasticity	49e9 MPa
Confining pressure	1 MPa
Deviator stress application rate	0.2 m/sec
Block width	80.e-3 m
Block height	150.e-3 m
Notch width	40.e-3 m
Notch height	70.e-3 m

Walls were used to constrain the margins. Confining stress was applied to all margins except part of one side, which was left constrained by negligible confining stress so as to simulate the margin and corner of a mine opening. A deviator stress was then applied to the upper and lower walls.

The block compressed elastically until the particle bonds began to fail. The response of the block to the applied deviator stress was then monitored from the progression of bond failures (figure 2) and from a graphical representation of deviator stress versus strain (figure 3). The elasticity compared well with the input modulus. Bonds between particles failed either by tension or shear, but tensile failures dominated.

Initial bond failures were located just below the corner and near the free vertical surface (figure 2). Failures then progressed diagonally downward about 30° from the free surface in a series of four elongat-

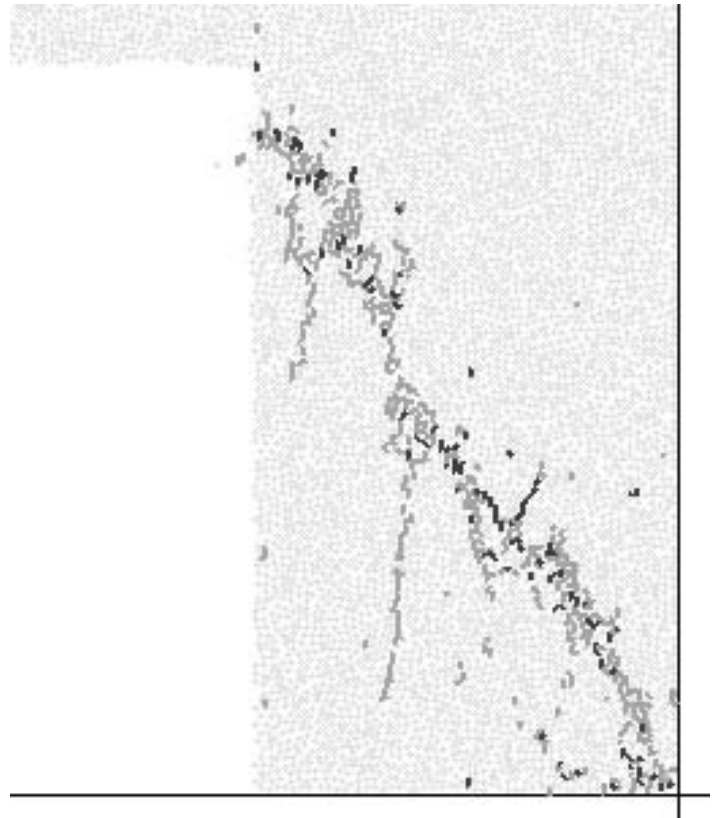


Figure 2.—Failed bonds at an advanced stage of block failure. Tensile failures are gray, shear failures black. Elongated en echelon clusters of tensile failures progressed from the upper left to the center of the block and finally merged into a continuous shear zone. Failures in the right half of the block progressed upward from the lower right corner and resulted from corner effects not related to the en echelon progression on the left.

ed clusters of tensile failures arranged in an echelon pattern. Discrete, individual fractures were not immediately evident, possibly reflecting a limitation of the method or of the input parameters used. In figure 2, the block is shown at a point in the simulation where extensive failure had occurred and where part of each individual cluster of tensile failures had been knitted together into a continuous shear zone. Two of the en echelon clusters near the sidewall ultimately merged into one discrete fracture that then propagated some distance below the corner. A deeper cluster also created a long discrete fracture. Failures in the right half of the block propagated upward from the lower right corner. These failures were attributed to corner effects not directly related to the failures in the left half of the block.

Figure 3 shows deviator stress and confining pressure on the block versus sample strain during the simulation. The initial steep slope indicates

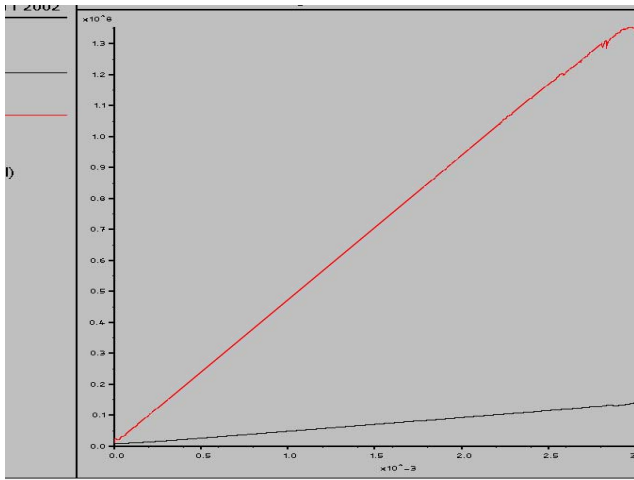


Figure 3.—Deviator stress-strain diagram showing initial elastic response and ultimate failure.

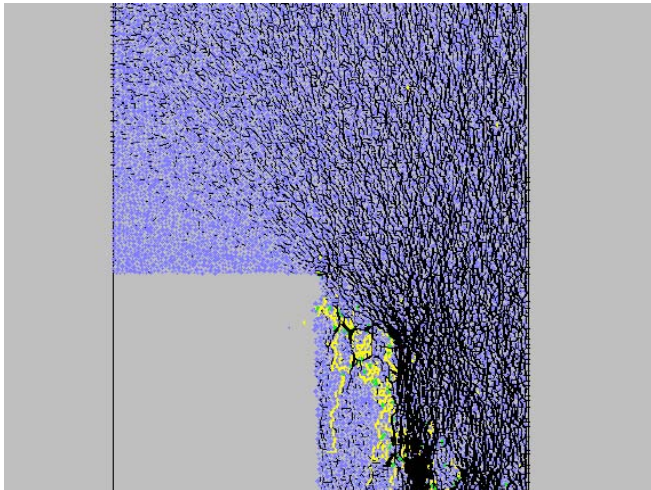


Figure 4.—Distribution of normal stresses after extensive deformation (black) showing destressed caused by fracture mechanism.

elastic compression, which is followed by instability and eventual failure. The lower line indicates the slight increase in confining pressure as the side walls locked as confining pressure was applied and deviator stress added.

In a separate plot showing the distribution of normal stresses after extensive deformation (figure 4), it is evident that the region adjacent to the opening became substantially de-stressed as a result of displacement involved with the fracturing. De-stressing and dilation of rock about openings as a result of fracturing in the excavation deformation zone are well known. Here the cause of de-stressing and dilation is identified as the fracture-forming mechanism; that is, shearing displacement and the

resulting fractures facilitated reduction in applied load at the expense of shear deformation and lateral dilation. White (2002) pointed out that such behavior may have major significance with respect to ground support practices involving placement of rock bolts.

Both FLAC and PFC modeling identified an initial tensile region near the corner and close to the surface of simulated, rectangular mine openings. FLAC suggested a mechanical reason for initiation of subsequent en echelon fractures as a result of redistribution of tension, and PFC verified the progression of en echelon fractures along a developing shear zone. The FLAC model indicated that the initial deformation of the rock and the appearance of tension did not involve the creation of microfractures, indicating that these are not essential elements of rock fracturing. However, microfractures would soften rock in areas of high shear strain and thereby concentrate strain and promote the formation of additional macrofractures at a lower level of stress than was used in the FLAC models.

5 SUMMARY

Based on these results, the following conclusions were reached.

- Elastic rock deformation about excavations generates local regions of tension.
- Tensile areas become sites of individual fractures, which must, therefore, be caused substantially by this tension.
- Tension is caused by elastic shearing displacement, which results in extension oblique to the plane of shearing.
- Fracture propagation redistributes tension in such a way as to cause the formation of en echelon fractures.
- Microcracks are not essential for the development of macrofractures, although microcracks would promote further deformation and thereby promote macrofracturing.
- Elastic displacement and the resulting fractures facilitate reduction in applied load at the expense

of shear deformation and lateral dilation, which has ground support implications.

- The mechanism described is probably active about excavations in both soil and rock.

6 REFERENCES

- Carter, B.J., Lajtai, E.Z., and Petukhov, A. (1991). Primary and remote fracture around underground cavities. *International Journal for Numerical and Analytical Methods in Geomechanics* 15: 21-40.
- Cloos, E. (1955). Experimental analysis of fracture patterns. *Bulletin of the Geological Society of America* 66: 241-258.
- Fairhurst, C., and Cook, N.G.W. (1966). The phenomenon of rock splitting parallel to the direction of maximum compression in the neighborhood of a surface. In Proceedings of the First Congress on the International Society of Rock Mechanics, Vol. 1. National Laboratory of Civil Engineering, Lisbon, Portugal, pp. 687-692.
- Fakhimi, A., Carvalho, F., Ishida, T., and Labuz, J.F. (2002). Simulation of failure around a circular opening in rock. *International Journal of Rock Mechanics & Mining Science* 39: 507-515.
- Francke, C.T., Terrill, L.J., and VandelKraats, J.D. (1997). Case study of the effect of stratigraphic locatoin on roof stability in rock salt. In Proceedings, 16th Conference on Ground Control in Mining, Morgantown, WV, pp. 243-250.
- Gay, N.C., and Ortlepp, W.D. (1979). The anatomy of a mining-induced fault zone. *Bulletin of the Geological Society of America* 90: 47-58.
- Hoek, E. (1964). Rock fracture around mining excavations. In 4th International Conference on Stratigraphic Control & Rock Mechanics, Columbia Univ., NY, pp. 334-348.
- Hoek, E., and Brown, (1980). *Underground Excavations in Rock*. Institute of Mining and Metallurgy, 527 pp.
- Itasca Consulting Group, Inc. (1993). Fast Lagrangian Analysis of Continua (FLAC) User's Manual. Minneapolis, MN.
- Itasca Consulting Group, Inc. (1999). PFC2D (Particle Flow Code in 2 Dimensions), Version 2.10. Minneapolis, MN.
- Kemeny, J.M., and Cook, N.G.W. (1991). Micromechanics of deformation in rocks. Toughening mechanisms in quasi-brittle materials, Kluwer, pp. 155-188.
- Lajtai, E.Z., Carter, B.J., and Ayari, M.L. (1900). Criteria for brittle fracture in compression. *Engineering Fracture Mechanics* 37(1): 59-74.
- Peng, S.S. (1976). A photoelastic coating technique for rock fracture analysis. *International Journal of Rock Mechanics, Mining Science, & Geomechanical Abstracts* 13: 173-176.
- Peng, S.S., and Johnson, A.M. (1972). Crack growth and faulting in cylindrical specimens of Chelmsford granite. *International Journal of Rock Mechanics & Mining Science* 9: 37-86.
- Segall, P., and Pollard, D.D., 1983, Joint formation in granitic rock of the Sierra Nevada. *Bulletin of the Geological Society of America* 94: 563-575.
- Stacey, R.R. (1981). A simple extension strain criterion for fracture of brittle rock. *International Journal of Rock Mechanics & Mining Science* 19: 469-474.
- Swanson, P.L. (1986). A fracture mechanics and nondestructive evaluation investigation of the subcritical-fracture process in rock. *Fracture Mechanics of Ceramics* 8: 299-317.
- Terrill, L.J., and VandelKraats, J.D. (1997). Case study of conditions observed during the removal of a highly fractured roof beam in bedded halite. In Proceedings, 16th Conference on Ground Control in Mining, Morgantown, WV, pp. 235-242.
- White, B.G. (2002). Shear mechanism for mining-induced fractures applied to rock mechanics of coal mines. In Proceedings of the 21st International Conference on Ground Control in Mining, Morgantown, WV, pp. 328-334.
- White, B.G., and Whyatt, J.K. (1999). Differential wall rock movements associated with rock bursts, Lucky Friday Mine, Coeur d'Alene Mining District, Idaho, USA. In Rock Mech. for Industry, Proceedings of the 37th U.S. Rock Mechanics Symposium, vol. 2, pp. 1051-1059.